FATIGUE CRACK PROPAGATION BEHAVIOR UNDER COMPLEX MODE LOADING

F. Hourlier, A. Pineau

Centre des Matériaux de
L'Ecole Nationale Supérieure des Mines de Paris
B.P. 87 - 91003 EVRY Cédex, France
Equipe de recherche associée au C.N.R.S. ERA767

ABSTRACT

Fatigue crack growth under cyclic mode I + steady mode II or III has been investigated on four materials. This complex mode loading gives rise to crack bifurcations, which can be explained by using a criterion which assumes that crack path corresponds to the direction where mode I fatigue crack growth rate is maximum.

INTRODUCTION

Some components, such as turbine shafts, are subjected both to a constant torque which provides the driving effort, and to an alternating bending stress which may arise from the weight of the rotor or from slight unavoidable unbalance. When a crack forms it generally initiates at the surface in a stress concentration zone and grows macroscopically in a transverse plane. Thus the crack is subjected to cyclic mode I loading plus steady mode III if it propagates in a radial direction or to cyclic mode I plus steady mode II if it grows in a tangential direction. The aim of this study was to investigate the effect of a superimposed steady mode II or III on fatigue crack propagation behavior.

There have been relatively few studies of fatigue crack growth rate (f.c.g.r.) under combined mode loading published in the literature. Most of those studies have emphasized the fact that fatigue cracks tend to propagate in a direction where mode I is predominant. In their investigation dealing with inclined cracks in panels of 7075T6 Al alloy Iida and Kobayashi (1969) observed that the crack bifurcated rapidly in a direction where K_I is maximum. In the same way, in a recent study by Pook (1977) dealing with mode II f.c.g.r. behavior of a mild steel it was observed that crack propagation occurs at an angle of roughly 70 degrees to the direction of precracking, that is in the direction supposed to be the one of mode I crack growth.

MATERIALS AND EXPERIMENTAL PROCEDURE

Mode I+III test materials were a titanium alloy TA5E ELI, an alloyed steel 26NCDV14 and a mild steel E36. The titanium alloy was heat treated at 1323K and it exhibited a coarse-grained acicular microstructure, with a grain size of about 700 µm.

Mode I+II tests were performed on an aluminium alloy 2024 T851. Specimens were cut from a 70 mm diameter bar. Chemical compositions and tensile properties of these materials are given in table 1.

Mode I+III tests

Notched round bars with dimensions as indicated in figure 1 were used for cyclic Mode I + steady mode III loading tests. All specimens were fatigue precracked under rotating bending at constant flexional displacement, using a modified lathe as a fatigue machine. By this technique, circular and well-centered cracks are easily obtained. Measurement of crack depth was performed with a DC potentiel drop technique. After precracking the specimens were loaded at 300K under cyclic tension with a superimposed steady torsion, with $R = K_{Imin}/K_{Imax} = .10$ and at a frequency of 20 Hz. Cyclic tension was applied by the actuator of a servohydraulic machine, whilst the steady torque was applied by using a dead weight loading.

The K_I and K_{III} stress intensity factors are given by Tada, Paris, Irwin (1973). Various values of K_{III}/K_{Imax} ratio between 0 and 2 were investigated for all three materials, the crack growth rate was extended from 10^{-6} mm/cycle to 10^{-3} mm/cycle. Full details of the experimental procedure are given by Hourlier, Pineau (1979).

Mode I+II tests

Cyclic mode I + steady mode II loading tests were performed on tubular specimens with a slot perpendicular to the axis (Fig. 1). The axis of the specimens was parallel to the longitudinal direction of the bar. Specimens were precracked under cyclic mode I at 300K at a frequency of 20 Hz, with a ratio R = 0,10. Afterwards they were subjected to cyclic tension and steady torsion, using the same test rig as employed for mode I+III loading. In order to calculate K_I and K_{II} the calibration curves by Erdogan and Ratwani (1972) were used. Buckling was avoided by using K_{II}/K_I ratio less than two. The effect of mode I + Mode II loading was investigated for f.c.g.r. within the limits of 10^{-5} mm/cycle and 10^{-3} mm/cycle.

TABLE 1 Chemical compositions and tensile properties of materials tested

TA5E ELI	Al	Sn	Si	Fe	O_2	N_2	C	$R_{0,2}$ MPa	R_m MPa	A %	Z %
	5,08	2,43	0,05	0,045	0,10	0,02	0,008	760	835	10	26
26NCDV14	C	Si	Mn	NL	Cr	Mo	V	789	875	18	69
	0,23	0,025	0,295	3,42	1,69	0,42	0,09				
E36	C	S	P	Si	Mn	N	Ti + Al	418	572	17	81
	0,179	0,016	0,014	0,426	1,415	0,005	0,002				
2024 T851	Cu	Mg	Si	Fe	Mn	Zr	Cr	465	515	4,5	30
	4,24	1,37	0,16	0,28	0,80	0,14	0,01				

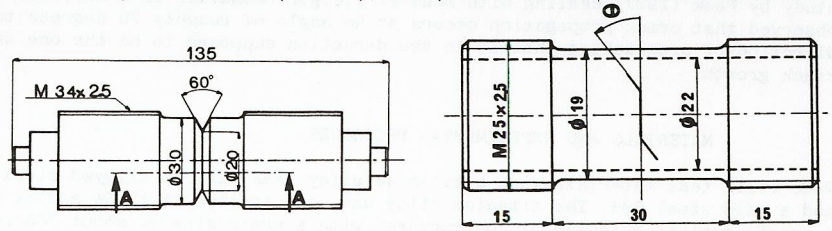

Fig. 1. Mode I+III and Mode I+II specimens

RESULTS AND DISCUSSION

FCGR behavior under Mode I + Mode III loading

It appeared that the superimposition of a constant torque (mode III loading) to the alternating tensile load (mode I loading) gives rise to strong effects, i.e.
- a decrease in fcgr which can reach two orders of magnitude;
- a significant macroscopic difference which appears on fracture surfaces.

The results concerning with f.c.g.r. under mode I+III loading have already been partly reported by Hourlier and Pineau (1978, 1979) for TA5E ELI alloy and 26NCDV14 steel. In this study similar effects have been observed on E36 steel. It was shown that the decrease in fcgr under mode I+III loading was associated to a closure phenomenom. In this paper the discussion deals only with the aspect of the fracture surfaces.

26NCDV14 steel. SEM observations of fracture surfaces at low magnification clearly show the differences between mode I and mode I + III (Fig. 2). Under mode I + III loading, ridges are observed running radially towards the center of the specimen. These features correspond to the formation of fairly regular sets of inclined facets, as shown schematically (fig. 3a) on a section AA defined in Fig. 1. It is worth noting that type A facets are slanting, whilst type B regions lay approximately in longitudinal radial planes. SEM observations at higher magnification indicate that type A facets display the same fractographic features as those observed in mode I loading whilst type B regions exhibit the features associated with ductile rupture and rubbing. Incompletely cracked specimens were sectionned along AA and longitudinally polished (Fig.3b). This micrograph shows that the part of the crack corresponding to mode I+III loading is divided into segments which are inclined to the tensile axis. These segments correspond to type A facets. Several sections carried out on the same specimen at increasing depths showed that the length of the ligaments left between type A facets could reach a few millimeters. It was noted that these ligaments which correspond to type B facets always had such an orientation that the applied torque pressed the new surfaces formed by the ligament rupture against each other. It is thought that this geometrical configuration in conjunction with the influence of the alternating tensile load could cause the strong rubbing effect observed on fracture surfaces.

The mean value $\bar{\alpha}$ of the angles formed by type A facets and transverse plane observed on several sections similar to that shown in Fig. 3b. was determined. The results given in Table 2 indicate that $\bar{\alpha}$ slightly increases as the value of the K_{III}/K_{Imax} ratio increases.

TA5E ELI. Alloy. Under mode I loading, because of its coarse grained microstructure, the crack path of this alloy deviated locally from the macroscopic crack plane which was always perpendicular to the tensile axis. This was especially marked in the low f.c.g.r. regime.

Under Mode I+III loading a significant macroscopic difference could be observed on the crack profiles. As in 26NCDV14 steel, sets of type A facets and regions B could be identified with naked eye. Sections of unbroken specimens revealed the same features as those observed in 26NCDV14 steel (Fig. 3c). The results giving the mean angles of deviation indicate that, for a given K_{III}/K_{Imax} ratio, the deviation is more important in this material than in 26NCDV14 steel (Table 2).

TABLE 2 Comparison of experimentally determined and calculated deviation angles.

Material	26NCDV14		TA5E ELI		E36
K_{III}/K_{Imax}	0,90	1,40	0,32	0,77	0,80
experimental α	6°	14°	17°	23°	≃0°
calculated α	14,5°	17,5°	15°	23°	≃0°

E36 Steel. Contrary to the other two materials, SEM observations showed that in this steel, fracture surfaces remained always perpendicular to the specimen axis, whatever the value of K_{III} applied to the specimens. In other words type A facets were not observed. However fracture surfaces still exhibited the features suggestive of a strong rubbing effect under mode I+III loading.

Fig. 2. 26NCDV14 Fractography (X22). From top to bottom, Mode I and Mode I+III loadings.

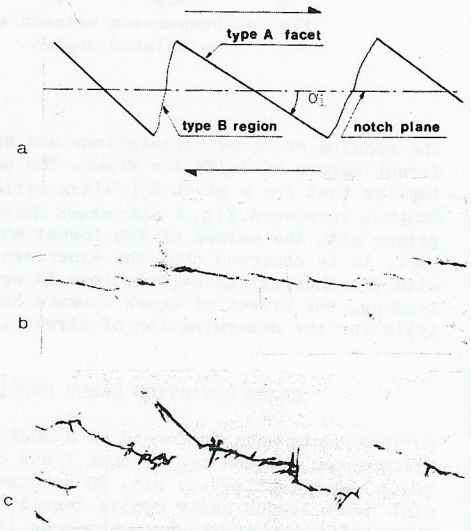

Fig. 3. Sections type AA.
a) Schematic.
b) 26NCDV14 (X14)
c) TA5E ELI (X10).

Discussion

The fractographic features observed in TA5E ELI alloy and in 25NCDV14 steel show a strong analogy with those reported by Sommer (1969). This author investigated the fracture of glass specimens subjected to monotonic mode I+III loading. In the fracture of glass the importance of the maximum tensile stress is well known. The superimposition of mode III loading rotates the maximum tensile stress away from the tensile axis. Thus if the crack tends to propagate in a plane perpendicular to the axis of the maximum principal tensile stress, the crack breaks into partial fronts which can adjust to the new tensile stress direction.

Unlike brittle fracture, in fatigue loading, the determination of the crack path must take into account not only the effect of the maximum tensile stress but also its amplitude. Under combined mode I + mode III loading the inclined type A facets correspond to the "twist" configuration, as defined by Lawn and Wilshaw (1975). These authors have shown that the stress intensity factors on a twisted facet inclined at an angle α can be calculated approximately as :

$$\Delta k_1(\alpha) = \Delta K_I(\cos^2\alpha + 2\nu\sin^2\alpha) \qquad (1)$$

$$k_{1max}(\alpha) = K_{Imax}(\cos^2\alpha + 2\nu\sin^2\alpha) + K_{III}\sin 2\alpha \qquad (2)$$

where ν is Poisson ratio. Very similar formulations can be derived for k_{III} and Δk_{III} stress intensity factors. If we assume that the local mode III component has no effect on the fatigue behavior - or, in other words, if we assume that fatigue cracking only occurs under the effect of local opening mode - the f.c.g.r. on a facet inclined at an angle α can be estimated by using the results obtained from mode I fatigue loading, i.e :

$$da/dN = f(\Delta k_1, k_{1max}) \qquad (3)$$

Several investigations have shown that in some cases the separate effects of K_I and K_{IMax} under mode I loading can be represented as :

$$da/dN = C(\Delta K_I)^{\beta}(K_{max})^{\gamma} \qquad (4)$$

where C is a constant for a given material. The values of β and γ for the three materials investigated are given in Table 3. The relationship (4) in addition to equations (1) and (2) enables to calculate the f.c.g.r. on a facet inclined at an angle α.

Let us assume that the crack propagates in the direction α where $da/dN(\alpha)$ is maximum. In the case of mode I+III loading this criterion implies that the angle is dependent on two parameters K_{III}/K_{IMax} and $\beta/\beta+\gamma$. For a material whose f.c.g.r. is dependent on K_{max} only, i.e. for $\beta = 0$, this criterion is the same as that of Erdogan and Sih ($\sigma_{\theta\theta max}$). On the contrary for a material which is not dependent on R ratio i.e. $\gamma=0$, this analysis predicts that $\alpha=0$ whatever the steady mode III applied.

TABLE 3 Values of β and γ of equation (4)

Material	β	γ	Validity range unit : m/cycle
TA5E ELI	3,05	1,75	$10^{-9} < < 5.10^{-6}$
26NCDV14	2,55	0,55	$5.10^{-9} < < 2.10^{-7}$
E36	3,04	≃ 0	$5.10^{-10} < < 2.10^{-7}$

In table 2, the α angle derived from this analysis can be compared to the values experimentally established. In TA5E ELI alloy the two sets of values are in good agreement, whilst in 26NCDV14 steel the predicted angles tend to be larger than the measured ones. It should be noted that for a given K_{III}/K_{IMax} ratio, the deviation

angle is larger in the titanium alloy as compared to 26NCDV14 steel, which is consistent with our criterion. Furthermore the fact that no deviation was observed in E36 steel is equally consistent with the absence of any significant effect of R ratio on the f.c.g.r. of this material, at least in the range of the f.c.g.r. investigated in this study.

However this analysis cannot predict the decrease in f.c.g.r. observed in cyclic mode I + steady mode III loading. As stated previously, this effect is mainly associated to a closure phenomenon which has not been taken into account in this study. Moreover it should be emphasized that the derivation of the stress intensity factors is very approximate for the complex tridimensionnal configurations corresponding to mode I + III.

FCGR BEHAVIOR UNDER MODE I + II LOADING

All tubular specimens were precracked under mode I in order to extent the slot. This extension always occurred perpendicularly to the axis of the specimen. The determination of the effect of R ratio on the f.c.g.r. of the Al alloy investigated in this part of this study was obtained by using CT type specimens. In the range of f.c.g.r. between 10^{-8} m/cycle and 10^{-6} m/cycle the data could be represented by the Paris relation :

$$R = 0.10 \qquad da/dN_{(m/cycle)} = 44{,}3.10^{-12} \, (\Delta K)^{3{,}04}_{MPa\sqrt{m}}$$

$$R = 0.50 \qquad da/dN_{(m/cycle)} = 17{,}4.10^{-12} \, (\Delta K)^{3{,}69}_{MPa\sqrt{m}}$$

The effect of R ratio is more important for relatively high f.c.g.r. than for lower f.c.g.r.

The superimposition of a steady mode II loading to cyclic mode I led to a deviation θ of the crack path as defined in fig. 1. It was observed that θ was an increasing function of K_{II}/K_{IMax} and of the f.c.g.r. which was measured on the kinked crack. Moreover, as in the case of mode I + III experiments, the superimposition of a steady torque gave rise to a decrease of f.c.g.r. This effect is believed to be associated with a crack closure phenomenom.

In order to interpret the observations concerning the deviation behavior the same type of criterion as used in the previous part was adopted. The stress intensity factors corresponding to a kinked crack have been determined by several authors. The most recent analysis by Amestoy (1979) indicates that an approximate solution derived from the Nuismer (1975) analysis which assumes the continuity of the tangential stress is numerically valid at least for $\theta < 45$ degrees. This simplified analysis can be used to derive the values of the stress intensity factors on a kinked crack, i.e. :

$$\Delta k_1(\theta) = \Delta K_I \cos^3 \theta/2 \qquad (5)$$

$$k_{1max}(\theta) = \cos^2 \theta/2 (K_{IMax} \cos \theta/2 + 3K_{II} \sin\theta/2) \qquad (6)$$

Here, it has equally been assumed that the f.c.g.r. behavior is dependent only on the local opening mode.

The values of angle θ corresponding to da/dN (θ) maximum were calculated by using equation (5) and (6) in addition to the Paris relations for R=0,10 et R=0,50.

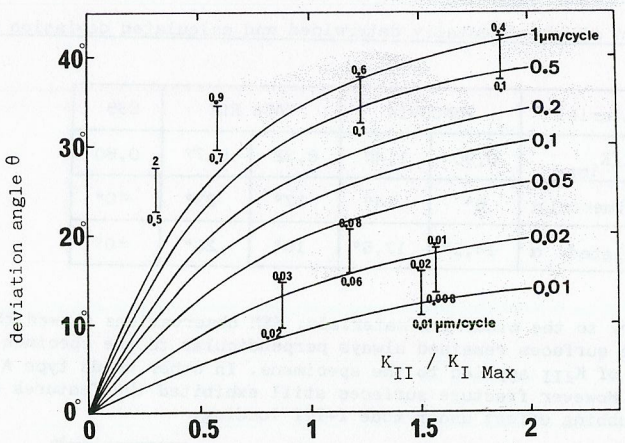

Fig. 4. Comparison between experimentally measured and calculated angles.

The results of these calculations are given in Fig. 4. Curves corresponding to different values of da/dN are drawn. The application of our criterion to this material implies that for a given K_{II}/K_{IMax} ratio, the deviation angle θ increases as the f.c.g.r. is increased. Fig. 4 also shows the values of θ angles experimentally defined together with the values of the lowest and the highest f.c.g.r. measured on the kinked part. It is observed that the experimental results are in reasonnable agreement with the theoretical calculations in spite of the fact that, as in mode I+III loading, the effect of crack closure has not been taken into account in this analysis for the determination of stress intensity factors.

CRACK DEVIATION UNDER CYCLIC MODE I + STEADY MODE II + III

Further tests were performed on a 2024 T851 Al alloy in order to investigate the differences between cyclic mode I and cyclic mode I + steady mode II + III. These tests had a qualitative aim. 20 mm diameter bars containing a transverse elliptical slot were loaded under cyclic tensile load or cyclic tension plus steady torque. This configuration was adopted because it could represent the behavior of a possible defect in a rotor.

It was observed that, unlike pure tensile loading which always gave rise to a propagation perpendicular to the tensile axis, the superimposition of a torque led to more complex fracture surfaces (Fig. 5). In the radial direction the macroscopic fatigue fracture plane remained perpendicular to the specimen axis but displayed ridges. SEM observations showed that these ridges were very similar to those observed in mode I+III specimens. On the edges of the specimens, the macroscopic fracture plane strongly deviated from the initial crack plane. This deviation is very similar to that observed in tubular specimens loaded under mode I+II. Several specimens were tested under loading conditions which produced various average crack propagation rates. It was noticed that the fractographic differences between mode I and mode I+II+III increase with the propagation rate. These further observations strongly support qualitatively at least, the analysis which has been proposed.

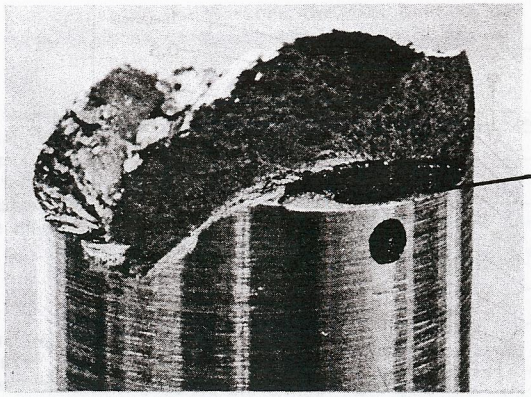

Fig. 5. Fracture surface of a 20 mm diameter bar with an elliptical transverse slot and loaded in cyclic tension plus steady torsion. Strong deviations are noted on the edges of the specimen.

SUMMARY AND CONCLUSIONS

A new criterion has been proposed to predict fatigue crack paths under cyclic mode I loading with a superimposed steady mode II or mode III loading. It has been shown that under complex mode loading a fatigue crack propagates in the direction in which the crack growth rate is maximum. The crack growth rate is assumed to be controlled only by the local mode I component . This analysis implies that the deviation behavior of a fatigue crack is not only dependent on the loading conditions but also on the fatigue crack propagation behavior of the material, especially its sensitivity to R ratio.

ACKNOWLEDGMENT

This study has been partly supported by D.G.R.S.T. Contrat n°77-7-0688.

REFERENCES

Amestoy, M., H.D. Bui and K. Dang-Van (1979). C.R. Acad. Sc. Paris 289 Série B., 99-102.
Erdogan, F., and M. Ratwani (1972). Int. Fracture Mechanics 8.
Hourlier, F., D. McLean and A. Pineau (May 1978). Metals Technology, 154-158.
Hourlier, F. and A. Pineau (Mars 1979). Mém. Scien. Revue Métallurgie, 175-185.
Hourlier, F. and A. Pineau (1979). Rapport final D.G.R.S.T.n° 77-7-0688.
Iida, S., and A.S. Kobayashi (Dec. 1969). Jal of Basic Engineering, 764-769 .
Lawn, B.R. and T.R. Wilshaw (1975). Fracture of Brittle Solids. Cambridge University Press.
Nuismer, R.J. (1975). Int. Jal of Fracture 11, 2, 245-250.
Pook, L.P. (1977). Int. Jal of Fracture 13, 867-868.
Sommer, E., (1969). Engineering Fracture Mechanics, 539-546.
Tada, H., P. Paris and G. Irwin (1973). The stress analysis of cracks handbook. Del Research Corp.